



#### Reaching new heights: A vertically-resolved ice nucleating particle 1

#### sampler operating on Atmospheric Radiation Measurement (ARM) 2

#### tethered balloon systems 3

- Jessie M. Creamean<sup>1</sup>, Darielle Dexheimer<sup>2</sup>, Carson C. Hume<sup>1</sup>, Maria Vazquez<sup>1</sup>, Benjamin T. M. Hess<sup>2</sup>, 4
- Casey M. Longbottom<sup>2</sup>, Carlos A. Ruiz<sup>2</sup>, Adam K. Theisen<sup>3</sup> 5
- 6 <sup>1</sup>Department of Atmospheric Science, Colorado State University, Fort Collins, Colorado, 80523, USA
- <sup>2</sup>Sandia National Laboratory, Albuquerque, New Mexico, 87123, USA 7
- 8 <sup>3</sup>Argonne National Laboratory, Lemont, Illinois, 60439, USA
- 9 Correspondence to: Jessie M. Creamean (jessie.creamean@colostate.edu)

#### 10 Abstract

- 11 Ice nucleating particles (INPs) are a rare yet climatically relevant subset of aerosols that initiate ice formation in mixed-phase
- 12 clouds, strongly influencing cloud microphysics, precipitation, and Earth's radiative balance. Despite their significance,
- ground-based measurements of INPs may not always be representative of those at cloud level, yet vertically-resolved INP 13
- 14 measurements remain limited. Here, we introduce PUFIN (Profiling Upper altitudes For Ice Nucleation), a robust,
- 15 lightweight INP sampler designed for routine deployment on the U.S. Department of Energy Atmospheric Radiation
- Measurement (ARM) user facility's tethered balloon system (TBS). PUFIN collects multiple filter samples per flight at up 16
- to three altitudes, integrating real-time monitoring of flow, power consumption, and atmospheric conditions, while remaining 17
- 18 fully operable from the ground. Multiple deployments at two ARM observatories in Maryland and Alabama demonstrate
- that PUFIN achieves sufficient aerosol loading to detect INPs down to  $\sim 10^{-3}$  L<sup>-1</sup> within as little as 28 minutes of sampling. 19
- 20 but typically within an hour. Data from recent deployments reveal altitude-dependent variability in INP concentrations,
- 21 indicative of boundary layer stratification and contributions from both local and transported aerosol sources. All resulting
- TBSINP data are publicly available via the ARM Data Center, and researchers may request PUFIN for future TBS campaigns
- 23 or access archived filters for additional analyses. Looking forward, routine PUFIN deployments can be used to enhance
- 24 understanding of the vertical distribution and seasonal variability of INPs, enabling improved representation of aerosol-cloud
- 25 interactions in Earth system models and advancing predictive capabilities for weather and climate.

#### 26 **Short summary**

22

- 27 PUFIN (Profiling Upper altitudes For Ice Nucleation) is a lightweight sampler flown on the U.S. Department of Energy's
- 28 Atmospheric Radiation Measurement user facility's tethered balloons to measure ice nucleating particles at multiple
- 29 altitudes. Deployments in Maryland and Alabama show it can detect low concentrations in under an hour and capture changes





with height. All data are publicly available, and future flights will help track seasonal and vertical patterns of these unique

31 particles.

### 1 Introduction

Ice nucleating particles (INPs) are a rare, but critical subset of atmospheric aerosols that catalyze the formation of cloud ice through heterogeneous nucleation, i.e., freezing supercooled liquid at temperatures above the homogenous threshold at roughly –38 °C (Pruppacher and Klett, 2010). Despite existing at concentrations orders of magnitude lower than cloud condensation nuclei (CCN) that facilitate the formation of cloud droplets, INPs exert an outsized influence on cloud microphysics, lifetime, and radiative properties (Kanji et al., 2017), especially in mixed-phase clouds, which are arguably the most prominent type of cloud globally (Mülmenstädt et al., 2015). By initiating the glaciation of such clouds, INPs can accelerate precipitation processes, alter cloud reflectivity, and modulate the hydrological cycle. Their role in determining cloud phase is especially consequential for Earth's energy balance, as ice-containing clouds differ strongly from liquid-only clouds in albedo and longwave emissivity (Storelvmo, 2017). Therefore, understanding INP abundance, composition, and variability is essential for improving the representation of aerosol-cloud interactions in weather and Earth system models (Burrows et al., 2022).

INPs connect boundary layer processes to terrestrial, oceanic, and cryospheric sources, linking biogeochemical systems to climate feedbacks on regional to global scales (Creamean et al., 2025b; Murray et al., 2021; Schnell and Vali, 1976; Steiner, 2020). However, INP measurements are often made at the surface, which may not accurately represent the concentrations or composition of INP populations at cloud level where ice nucleation processes occur, and are only directly relevant when clouds are coupled to the surface (e.g., Griesche et al., 2021). Furthermore, the types of INPs often vary with altitude. A recent modeling study suggests that, on a global average, biological and marine organic INPs are more prevalent at lower altitudes depending on hemisphere and freezing temperature, whereas dust INPs dominate at higher altitudes (Chatziparaschos et al., 2025). While crewed aircraft have a long history of conducting airborne INP measurements, they typically provide only brief snapshots and often cannot sample close enough to the surface to capture the full vertical structure from the ground to cloud base.

Smaller platforms such as uncrewed aerial and tethered balloon systems (UASs and TBSs, respectively) help fill this gap. Although these systems cannot accommodate the larger payloads of crewed aircraft, advances in lightweight instrumentation now enable vertically-resolved comprehensive measurements of meteorology and aerosol properties (Dexheimer et al., 2024; Mei et al., 2025; Pohorsky et al., 2024; Pilz et al., 2022). TBSs are particularly valuable because they can provide routine profiling or sustained sampling of aerosols at targeted altitudes up to several hours, reaching up to 1–2 km above ground level, below, into, and above clouds (e.g., Creamean et al., 2021). These capabilities offer certain advantages over UASs, which are frequently limited by line-of-sight or altitude regulations, payload weight restrictions depending on aircraft design,





and relatively short flight times at often an hour or less. Recent studies such as Pilz et al. (2023, 2024) and Londardi et al. (2022) reported aerosol observations from TBS platforms during summer of the 2019–2020 Multidisciplinary drifting Observatory for the Study of Arctic Climate (MOSAiC) expedition. Their results revealed substantial complexity in aerosol vertical structure, which varied by day and airmass origin, though most profiles indicated new particle formation above low-level clouds. Similarly, Guy et al. (2024) measured aerosol size distributions from the surface to cloud base over the central Greenland Ice Sheet using TBS and found distinct stratification, concluding that surface measurements alone failed to represent cloud-relevant aerosol conditions roughly half of the time. Pohorsky et al. (2025) also observed distinct aerosol layering using TBS in a high-latitude urban environment, where heavy pollution was trapped beneath a strong temperature inversion and overlain by typical Arctic haze aerosols. In another study, Zinke et al. (2021) developed a cloud water sampler they deployed on a TBS, enabling measurements of bulk cloud residual chemical composition and INP concentrations in the high Arctic from an icebreaker, although these were not vertically-resolved.

Only a limited number of studies have reported on vertically-resolved INP measurements from balloon platforms. Creamean et al. (2018) quantified INPs in both immersion and deposition modes across six altitude ranges during three test flights in

et al. (2018) quantified INPs in both immersion and deposition modes across six altitude ranges during three test flights in Colorado, using launched balloons rather than a TBS. This approach was challenging, as launched balloons can be entrained in low-level jets carrying them long distances, and physical retrieval is required to collect filters for offline INP analysis. Porter et al. (2020) developed a size-resolved sampling payload for offline INP analysis, the SHARK (Selective Height Aerosol Research Kit), for deployment on a TBS. This system has been tested at several locations, including in the high Arctic (Porter et al., 2022); however, it collects samples at only one altitude above ground level per flight. More recently, Böhmländer et al. (2025) developed an INP sampler capable of collecting filters at multiple altitudes for offline analysis. The system was initially tested on a UAS in Finland, with plans to test it for TBS applications. While these previous studies mark important progress toward resolving the vertical distribution of INPs, substantial effort is still needed to establish reliable, routine measurements. Such advancements are essential for improving the representation of INPs in models and, consequently, the simulation of aerosol-cloud interactions across vertical scales.

Here, we present a robust INP sampling system designed to address this gap, called PUFIN: Profiling Upper altitudes For Ice Nucleation. The instrument collects filters at up to three distinct altitudes plus a blank during each TBS flight and can be fully controlled from the ground. Developed collaboratively by the INP and TBS instrument teams under the U.S. Department of Energy's Atmospheric Radiation Measurement (DOE ARM) user facility, the system is intended for routine deployment at ARM sites in response to user requests. Resulting data products are publicly released on the ARM Data Center (<a href="https://www.arm.gov/data">https://www.arm.gov/data</a>) within six months of each TBS campaign. In this paper, we describe the system design and flight operations, outline the offline sample processing and data production, summarize the data that are currently available and how to access them, and guide users how to request deployment of PUFIN for their own research needs.



92

93

94 95

96

97

98

99

100

101

102

103

104

105

106107

108109

110



# 2 Instrument description

#### 2.1 DOE ARM TBS and INP initiatives

The ARM TBS program has evolved into a critical observational capability for capturing high-resolution, vertically-stratified atmospheric data, operating at ARM observatories using helium-filled Skydoc balloons capable of ascending to approximately 1.5 km above ground level. Typically, ARM conducts six to eight two-week TBS missions each year, with flights deploying baseline instrumentation suites, including aerosol, thermodynamic, and turbulence sensors, tailored to research objectives across clear-air and, occasionally, in-cloud conditions. More details on the TBS system and standard instrument payload can be found in Dexheimer et al. (2024) and up-to-date information on the ARM TBS website (https://www.arm.gov/capabilities/instruments/tbs).

Since 2020, ARM has provided routine, publicly-available INP measurements at select sites. Prior to that, INP sampling was considered a guest instrument activity and required proposals by researchers for targeted campaigns and locations. Demand for such measurements has since grown, and as of 2025 INP data are available from seven ARM sites. These data are generated by collecting filters at ARM fixed observatories and mobile facilities, followed by offline processing with the Ice Nucleation Spectrometer (INS) at Colorado State University (CSU), as described briefly below and in detail in Creamean et al. (2024, 2025a). Data products can be accessed through the ARM Data Center by searching for "INP." Up-to-date information, including deployment details and data availability from TBS operations, is provided on the ARM INS website (https://www.arm.gov/capabilities/instruments/ins), where a routinely updated field log is also available for community reference.

## 2.2 Design and integration of PUFIN with the TBS

111 PUFIN operates similarly to the standard ARM INP sampling system, but on a smaller scale and with multiple filters attached. 112 A detailed parts list and design schematic are publicly available on GitHub at https://github.com/ARM-Development/TBS-INP-Design to enable researchers to build and deploy their own PUFIN replicas for their independent or collaborative studies. 113 Figure 1 illustrates PUFIN's flow diagram, which includes a dry floating scroll pump (SVF-E0-50P, ScrollLabs<sup>®</sup>), a multi-114 gas flow sensor (SFM4300, Sensirion AG), four stainless steel solenoid valves (PL-220101, Plum Garden), and four ports 115 116 for reusable 47-mm in-line polycarbonate filter holders (Pall Life Sciences). The pump features a brushless motor powered by 24 VDC, achieves an ultimate vacuum of <1 mbar, and provides flow rates up to 50 sL min<sup>-1</sup> without a filter attached. 117 118 The flow sensor operates over a 0-50 sL min<sup>-1</sup> range. Each solenoid valve, with \(\frac{1}{4}\)-inch threaded inlet connections, requires 119 12 VDC and is controlled via a motor driver controller board (L298N, HiLetGo). The filter holders, with an effective filtration 120 area of 9.6 cm<sup>2</sup>, are prepared as outlined in Section 2.4.1. With prepared filter holders attached, the pump can pull a maximum 121 of roughly 11 sL min<sup>-1</sup> through the standard 0.2-µm pore size filters used for the ARM INP measurements. Connections at 122 both ends consist of 1/4-inch hose barb adapters, linking to 1/4-inch tubing inside PUFIN and opening directly to the air on the





exterior (Figure 2). PUFIN's components are protected by a 3D-printed enclosure, which is equipped with a ventilation fan for in-flight cooling and backed with a 0.32 cm thick aluminum electrical ground distribution board that also provides structural integrity for the mounting point to the tether. The enclosure and all other 3D-printed parts are fabricated from white ASA (acrylonitrile styrene acrylate) polymer (Bambu Lab) due to its exceptional UV and temperature resistance, high impact strength, durability, and suitability for long-term outdoor use. The total flight-ready weight of the instrument is 6.1 kg.

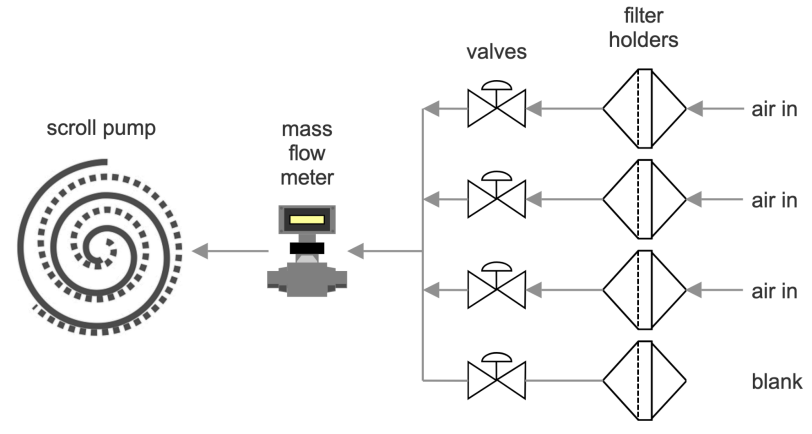


**Figure 1:** Schematic of PUFIN airflow. Main components are labeled. Valves are sequentially triggered to direct airflow through one filter at a time, while the fourth filter serves as a field blank and remains closed to airflow. Arrows indicate direction of airflow. The schematic was generated with SmartDraw.com.

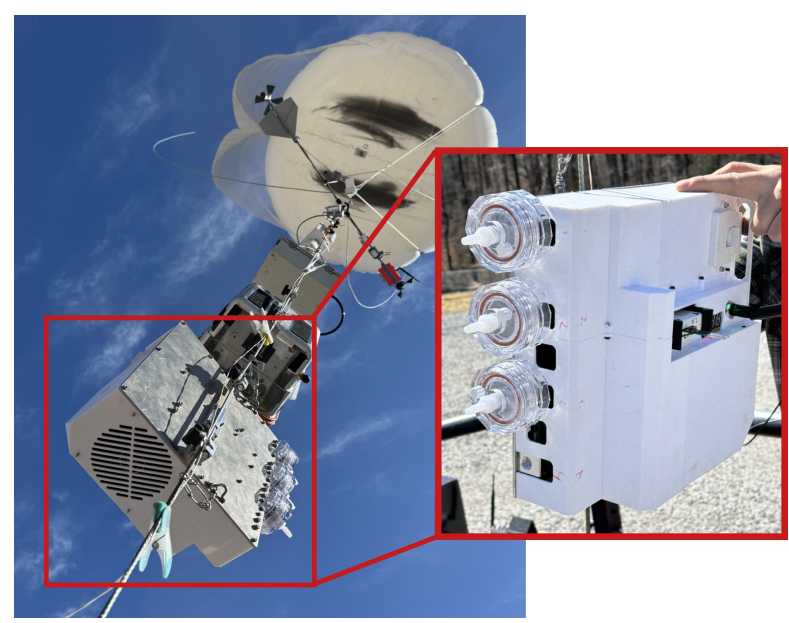


**Figure 2:** Exterior views of PUFIN mounted on the ARM TBS tether during a field deployment, shown in flight alongside other instrument payloads. The inset on the right displays a frontal view of PUFIN with filter holders attached. This flight required collection of INPs at two designated altitudes plus one field blank.



138139

140141

142

143

144

145

146

147148

149

150

151

152

153

154

155

156

157

160



Figure 3 illustrates the primary components and features of both the interior and immediate exterior of PUFIN. It is powered by a 28.8-V, 14,000-mAh lithium ion battery pack (8S4P, MaxAmps), housed within a 3D-printed enclosure for protection and secure mounting. The battery pack typically powers PUFIN for approximately 3.5 hours depending on the target flow rate, ambient temperature, and air density. A 30-W DC/DC converter (PYB30-U, Bel Power Solutions) steps down the battery voltage to 12 V to supply the pump, valves, and sensors. System power consumption is monitored using a current, voltage, and power monitor (INA260, Adafruit Industries LLC), providing measurements of electrical load and enabling safe operation during flight. PUFIN's control system is built around a TEENSY 4.1 microcontroller (iMXRT1062, SparkFun Electronics), which serves as the central processing unit for all sensor operations. Onboard sensors communicate digitally with the microcontroller, and analog pump command signals are generated using a digital-to-analog converter (MCP4725, SparkFun Electronics), enabling the microcontroller and other computational components to interpret and respond to sensor inputs accurately. This configuration allows precise regulation of flow rates, valve actuation, and system monitoring during flight. PUFIN's communications system integrates atmospheric sensing, data transmission, and user interface components to enable real-time monitoring during flight. An iMet-XQ2 sensor measures atmospheric pressure, temperature, and humidity, and includes a GPS receiver, rechargeable battery, and onboard data logger. The sensor is mounted in a custom 3D-printed holder bracket. Wireless data transmission is achieved via a 2.4-GHz radio frequency transceiver module with antenna (NRF24L01P+PA+LNA, HiLetgo), allowing real-time communication between PUFIN and the ground station. A 9-dBi omni-directional antenna is used with the transceiver to increase range (ANT-WS-A-NF-09-150, ATOP Technologies). System status and measurements are displayed locally on a 2.8-inch LCD touch panel (ILI9341, HiLetgo) and a digital LED tube clock module. All remote electronics, including the transceiver, display, and sensor assemblies, are housed in a series of 3D-printed enclosures to protect components while maintaining accessibility and visibility during deployment.

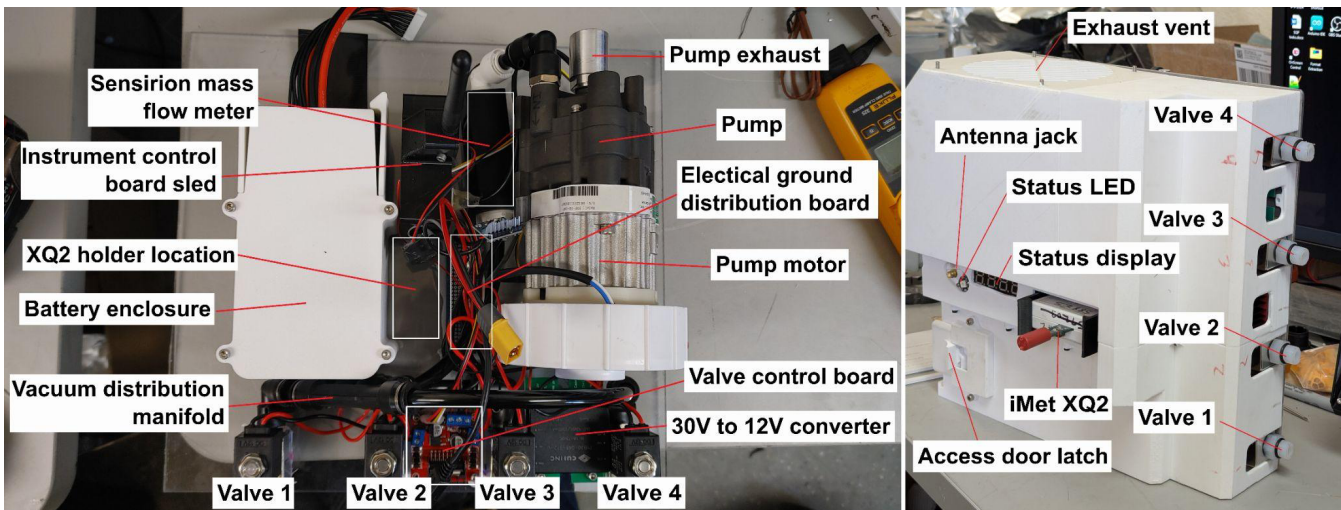


Figure 3: Photos of the interior (left) and immediate exterior (right) of PUFIN. The main components and features are labeled. The exterior housing shown in the right image is-3D printed.





# 2.4 INP sample collection during deployments

#### 2.4.1 Filter holder preparation

In preparation for aerosol collection, 0.2-μm polycarbonate filters (47-mm diameter Whatman® Nuclepore<sup>TM</sup> Track-Etched Membranes) are loaded into the reusable 47-mm polycarbonate in-line filter holder, pre-cleaned with cycles of methanol and deionized water. These filters are identical in preparation to those used at ARM fixed and mobile sites (Creamean et al., 2025a). All components, including filters, forceps, and workspaces are pre-cleaned following the procedure described in Barry et al. (2021). Filter holders are disassembled and reassembled under ultraclean conditions inside a laminar flow cabinet with near-zero ambient particle concentrations, wrapped in foil, then sealed and stored individually in clean airtight bags until deployment. Filter holders are thoroughly cleaned following each use and before reuse by immersion in 5% hydrogen peroxide for 1 hour, followed by 10 minutes of ultra sonication in deionized water and Windex® Original Glass Cleaner to remove any remaining particles.

## 2.4.2 Operation of PUFIN during flight

PUFIN is typically operated manually unless used in environments with elevated electromagnetic interference. During setup, the blank filter remains installed as the instrument is mounted onto the tether. It is then removed using latex gloves, wrapped in aluminum foil, labeled, and stored in a –80 °C ultracold freezer. The pump is activated, and the first solenoid valve is manually opened to begin sampling (Figure 4). The instrument makes multiple passes through the first target altitude over a 30–60 minute interval. Before transitioning to the next altitude range, the valve is closed, and the next solenoid valve is opened. This process is repeated for the third valve at the highest altitude. After the flight, the instrument is removed from the tether and placed on a workspace lined with clean aluminum foil. Filters are removed using latex gloves, wrapped in foil, labeled, and stored in the same plastic bag as the blank filter in the –80 °C freezer. The operation log is retrieved from the onboard SD card. Once all flights are completed, the collected filters are shipped overnight to CSU for analysis in a hard-sided 7 kg-capacity cooler with 2.2 kg of dry ice.







**Figure 4:** Photo of the PUFIN ground station undergoing manual operation. The image depicts the pump motor in an inactive state ('DISABLED') with all four valves closed and 0 sL min<sup>-1</sup> of flow. The target flow upon activation is 5.00 sL min<sup>-1</sup>.

## 3 Filter processing for INP data

## 3.1 INS sample processing

The INS, similar to the CSU Ice Spectrometer, simulates immersion freezing of cloud droplets by measuring heterogeneous ice nucleation initiated by ambient aerosol particles acting INPs (Creamean et al., 2024, 2025a). This technique provides quantitative insight into the population of ambient aerosols capable of initiating cloud ice formation across a broad range of subzero temperatures, thereby determining INP concentrations spanning up to six orders of magnitude. The INS is supported by robust experimental protocols and has been widely applied across diverse atmospheric contexts (e.g., Barry et al., 2023; Beall et al., 2017; DeMott et al., 2017; Hill et al., 2016; Hiranuma et al., 2015; Lacher et al., 2024; McCluskey et al., 2017; Suski et al., 2018).

The INS contains two units that operate simultaneously to increase processing throughput. Each unit consists of two 96-well aluminum incubation blocks designed for polymerase chain reaction (PCR) plates, arranged end-to-end and thermally regulated via cold plates on the sides and base. The instrument measures freezing across a temperature range of 0 °C to approximately –27 to –30 °C. For analysis, filters are carefully removed from the in-line holders under ultraclean conditions inside a laminar flow cabinet. Each filter is placed in a sterile 50 mL polypropylene tube with 7–10 mL of 0.1 µm-filtered deionized (DI) water, with the volume adjusted based on expected aerosol loading; lower volumes are used for cleaner environments to enhance sensitivity. Samples are re-suspended by end-over-end rotation for 20 minutes. Serial dilutions are prepared using the suspensions and 0.1 µm-filtered DI water, typically including 11-fold dilution steps. Each suspension and its dilutions are aliquoted into sets of 32 wells (50 µL per well) of single-use 96-well PCR trays (Optimum Ultra), along with a 32-well negative control containing only filtered DI water. Trays are placed into the INS blocks and cooled at a controlled





rate of 0.33 °C min<sup>-1</sup>. Uncertainty of the thermocouple is ±0.2 °C. Freezing is monitored optically using a CCD camera with a 1-second resolution. A continuous flow of HEPA-filtered N<sub>2</sub>, precooled just above block temperature, purges the headspace to minimize condensation and prevent warming of the samples. Field blanks are processed in an identical manner as sampled filters.

## 3.2 INP concentration and uncertainty calculations

- 210 INP concentrations, blank corrections, and uncertainties were generated using the Open-source Library for Automating
- Freezing Data acQuisition from Ice Nucleation Spectrometer (OLAF DaQ INS; https://github.com/SiGran/OLAF). Details
- are described in Creamean et al. (2025a). The program calculates INP concentrations at each temperature interval using the
- fraction of frozen droplets and the known total volume of air that passed through each filter, following Equation (1) (Vali,
- 214 1971):

209

- 215  $K(\theta)(L^{-1}) = -\frac{\ln(1-f)}{Vdrop} \times \frac{Vsuspension}{Vair}$
- 216 (1)

225

226

- where f is the proportion of frozen droplets,  $V_{drop}$  is the volume of each droplet,  $V_{suspension}$  is the volume of the suspension,
- and  $V_{air}$  is the volume of air sampled (liters at standard temperature and pressure (STP) of 0 °C and 101.32 kPa). The primary
- variable of the INS is the freezing temperature spectrum of cumulative immersion mode INP number concentration,  $K(\theta)$ ,
- from aerosols re-suspended from individual filters. INP spectra are corrected using DI negative controls and subsequently
- blank-subtracted. Binomial 95% confidence intervals are calculated following Agresti and Coull (1998), varying with the
- proportion of wells frozen. For example, freezing in 1 of 32 wells yields a confidence interval range of approximately 0.2–
- 5.0 times the estimated concentration, while 16 of 32 yields approximately 0.7–1.3 times the estimated concentration.  $K(\theta)$
- and upper and lower confidence intervals are derived per every 0.5 °C interval.

# 4 Accessibility of PUFIN and resulting TBSINP data

# 4.1 Availability of TBSINP data and filters

- 227 INP data collected with PUFIN on the ARM TBS and processed using the INS are available through the ARM Data Center
- by searching for "TBSINP". Not all TBS deployments included PUFIN and resulted in TBSINP data, but this section
- summarizes those that have. Table 1 provides an overview of TBS campaign details through the end of 2025, which occurred
- at four main ARM sites: 1) Southern Great Plains (314 m AMSL, 36.607° N, 97.488° E), 2) Gunnison, Colorado (2886 m
- AMSL, 38.956° N, 106.988° W) during the SAIL (Surface Atmosphere Integrated field Laboratory) campaign, 3) Bankhead
- National Forest, Alabama (293 m AMSL, 34.342° N, 87.338° W), and 4) Baltimore, Maryland (158 m AMSL, 39.422° N,
- 233 77.21° W) during the CouRAGE (Coastal-urban-Rural Atmospheric Gradient Experiment) campaign. While not all datasets
- are available, those pending release as of the publication date of this paper are indicated in the table. Campaigns that used an





earlier INP collection method predating PUFIN (called the IcePuck), as described in Creamean et al. (2024), are also identified. Limitations of the IcePuck in collecting sufficient air volumes to capture the warmer freezing temperature range of the cumulative INP spectrum, along with challenges in ease of use, prompted the development of PUFIN. Exact start and end dates and times, altitude range, sample duration, and volume of air sampled for each sample and each flight can be found in the field log link on the INS website (<a href="https://www.arm.gov/capabilities/instruments/ins">https://www.arm.gov/capabilities/instruments/ins</a>). For deployments in which data are not or only partially available, researchers interested in accessing or analyzing these samples may submit a request to ARM (<a href="https://www.arm.gov/guidance/campaign-guidelines/small-campaigns">https://www.arm.gov/guidance/campaign-guidelines/small-campaigns</a>). User-requested data from additional INP processing will also be made accessible to the broader research community through the ARM Data Center.

**Table 1.** Details on ARM TBS deployments with INP sampling. Information includes ARM sampling site, flight dates during each deployment, altitude range of the flights (meters above mean sea level), the range of sample duration (minutes), range of volume of air collected per sample (liters), if the data are available on the ARM Data Center (ADC), and the sampling method used. For the site, SGP = Southern Great Plains, GUC = Gunnison, Colorado, BNF = Bankhead National Forest, Alabama, and CRG = Baltimore, Maryland. Sampling method indicates whether the older INP sampler (IcePuck) or PUFIN were used. For data availability, yes = all data are posted, partial = some data are available within the dates indicated, queued = samples will be processed / data will be available in the future, and no = samples are archived for possible future processing / no data are available.

ARM site	Flight dates	Altitude range (m AMSL)	Sample duration (min)	Vol air sampled (L)	Data on ADC	Sampling method
SGP	10 – 26 Apr 2022	0 – 1000	30 – 150	34 – 133	Yes	IcePuck
GUC	6 – 16 May 2022	0 - 500	74 – 149	40 – 90	Yes	IcePuck
GUC	23 – 28 Jul 2022	0 - 750	21 – 119	27 – 71	Partial	IcePuck
GUC	21 – 24 Jan 2023	0 – 560	33 – 74	30 – 37	No	IcePuck
GUC	6 – 11 Apr 2023	0 – 1150	70 – 120	34 – 133	Partial	IcePuck
GUC	9 – 13 May 2023	0 – 500	119 – 120	30 – 41	No	IcePuck
GUC	9 – 15 Jun 2023	0 – 1000	60 – 120	16 – 47	No	IcePuck
CRG	14 – 23 Feb 2025	0 – 900	59 – 119	447 – 1456	Yes	PUFIN
CRG	15 – 28 Jul 2025	0 – 1050	4 – 30	31 – 245	Yes	PUFIN
BNF	21 – 27 Mar 2025	0 – 1100	60 – 91	416 – 1157	Yes	PUFIN
BNF	17 – 27 Apr 2025	0 – 850	46 – 62	350 – 438	Yes	PUFIN
BNF	29 May – 6 Jun 2025	0 - 700	28 – 44	204 – 394	Yes	PUFIN
BNF	9 – 24 Aug 2025	0 – 850	30 – 89	254 – 713	Queued	PUFIN





The SGP site is located in the midst of agricultural fields in north-central Oklahoma, United States, which often produce high concentrations of INPs from soil dust lofted during farming activities such as harvesting and plowing (Knopf et al., 2021). The TBS deployment at SGP was part of an intensive observational period (IOP) aimed at investigating the drivers of variability in INP concentrations from regional emissions of fertile, organic-rich agricultural soils, as well as intermittent contributions from other sources, including aerosols from controlled burns or wildfires, long-range transported desert dust, cellulose-containing plant matter, fungal spores, and microbial particles. Cornwell et al. (2024) reported enrichments of phosphate, lead, and soil organics in dust particles acting as INPs from surface measurements, while non-ice-nucleating aerosols were primarily carbonaceous or secondary in origin. TBSINP data from this deployment are still under analysis for a forthcoming publication, but several noteworthy case days have already emerged, including instances with elevated particle concentration layers within the boundary layer. The GUC site, part of the SAIL campaign, is located high in the Colorado Rocky Mountains. SAIL aimed to develop a quantitative understanding of atmospheric and land–atmosphere interaction processes, across relevant scales, that influence mountain hydrology in the midlatitude continental interior of the United States (Feldman et al., 2023). TBS flights at GUC were conducted in all seasons except autumn and sampled both within the mountain valley and above ridgelines, capturing cases influenced by local valley sources as well as more regional aerosol below cloud level.

In this paper, we focus on the TBS deployments at CRG and BNF where PUFIN was included, and consequently, larger air volumes were collected (Table 1). These conditions produced relatively complete cumulative INP spectra over much shorter collection times (~30 to 60 minutes) compared with previous IcePuck deployments at SGP and GUC (Figure 5), which often required more than an hour to obtain sufficient sample loading for INP detection, given the low flow rate of IcePuck. The shorter collection time is advantageous because it allows sampling at more altitude ranges per flight given constraints on flight duration imposed by battery life and staffing limitations. However, Figure 5 also includes data from SGP and GUC sites, so some of the observed variability likely reflects the distinct aerosol loadings characteristic of each location.





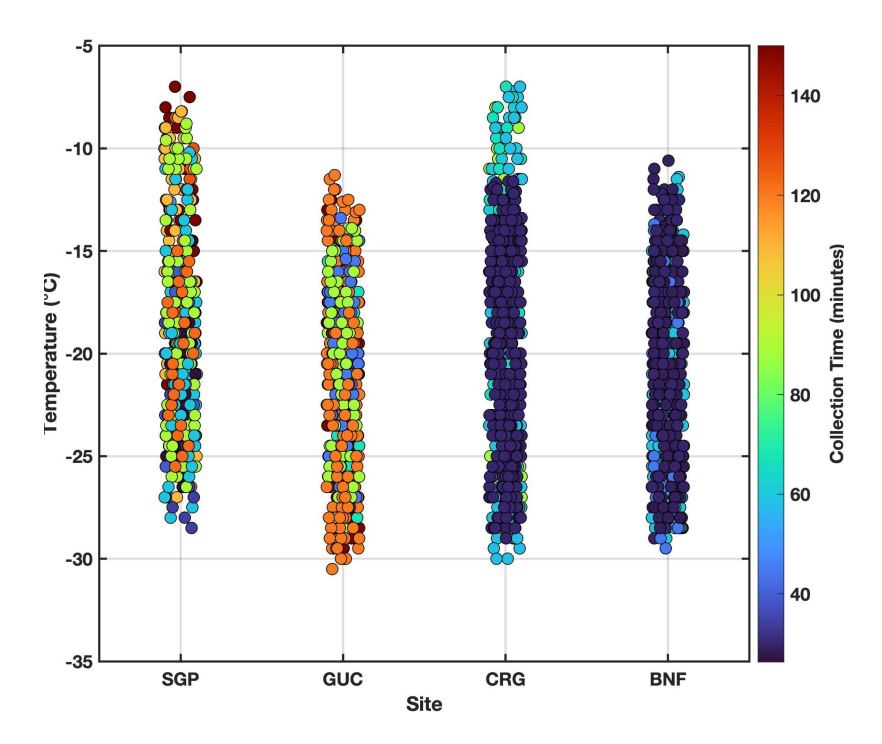


**Figure 5:** Temperatures at which INPs were detected with the INS across all altitude ranges at the four sites with TBS deployments. Data points are colored by sample collection time (minutes). SGP and GUC samples were collected using the IcePuck, requiring longer sampling durations, whereas CRG and BNF samples were collected with PUFIN, allowing shorter collection times.

At CRG, TBS operations took place in both winter and summer as part of the CoURAGE campaign, which investigates how spatial gradients in land–atmosphere interactions across coastal, urban, and rural environments influence atmospheric processes such as aerosols, clouds, radiation, precipitation, and boundary-layer dynamics in the Baltimore region. A central objective of CoURAGE is to improve representation of coastal urban climates in Earth system models by leveraging observations from a four-node regional observatory network to test and refine model simulations of urban atmospheric environments. The BNF observatory, a long-term ARM mobile facility (AMF) located in northwest Alabama, United States, is designed to advance understanding of the coupled interactions among aerosols, clouds, and land–atmosphere processes, particularly within forested environments, to strengthen their representation in Earth system models. In addition, BNF is envisioned to serve as a testbed for applying artificial intelligence and machine learning methods to enhance predictability in atmospheric science, while supporting detailed studies of land–atmosphere feedbacks and aerosol–cloud interactions. To date, four TBS deployments have been conducted at BNF during spring and summer, with additional campaigns anticipated in the future.



290

291

292

293

294

295

296

297

298

299300

301

302

303

304305

306307

308309

310



# 4.2 INP profile data from recent ARM TBS campaigns

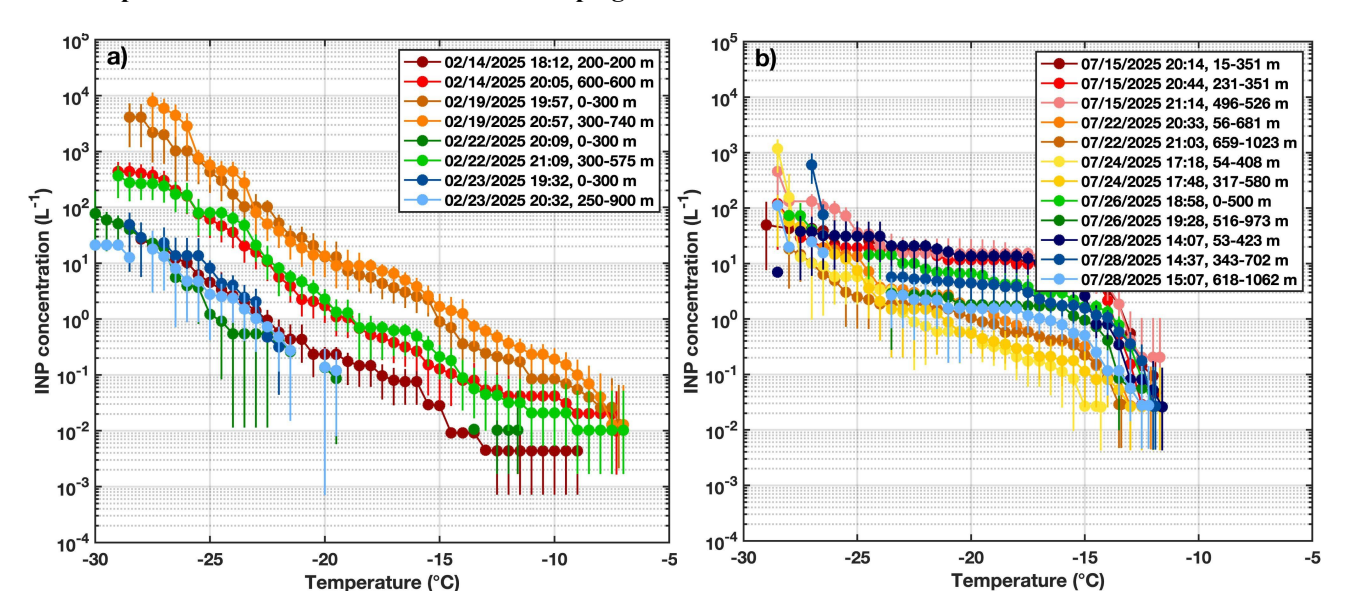


**Figure 6:** Cumulative INP spectra from CRG TBS flights in a) February and b) July 2025. Two altitudes or altitude ranges were sampled per day. PUFIN loitered at a single altitude if the range is the same value; if a range with different values is listed, PUFIN profiled within that range to collect the sample. Date (mm/dd/yyyy) and time (hh:mm:ss) indicate the sampling (flight) start in UTC. Each day is a different color, with each altitude (range) a different shade of that color. Error bars indicate 95% confidence intervals.

Figure 6 shows cumulative INP spectra from CRG during February and July 2025, with darker shades of each color representing the lower altitude sampled each day. In February, multiple flights were conducted, with two altitudes sampled per day, revealing substantial variability both in overall INP concentrations and in the vertical structure. For example, on 14 and 22 February (red and green shades, respectively), higher altitudes (loitering at 600 m and 300-575 m, respectively) consistently exhibited statistically significant elevated INP concentrations (two-sample t-test; p < 0.02) across all temperatures compared with lower altitudes (200 m and 0-300 m, respectively). In contrast, on 19 and 23 February (orange and blue shades, respectively), no statistically significant differences (p > 0.07) were observed between upper and lower altitude levels (0-300 m versus 300-740 m and 0-300 m versus 250-900 m, respectively), as concentrations overlapped within the 95% confidence intervals. These results suggest differences in boundary layer stratification and/or the presence of transported aerosol layers aloft with higher INP abundances on 14 and 22 February, whereas conditions on 19 and 23 February were more consistent, likely with a more well-mixed boundary layer. In July, INP concentrations averaged an order of magnitude lower (19 L<sup>-1</sup>) than in February (145 L<sup>-1</sup>) at -25 °C, but were an order of magnitude higher at -15 °C (3 versus 0.6 L<sup>-1</sup>). Interestingly, even the sample collected over just 4 minutes (31 L of air) yielded detectable INP concentrations and was among the higher values observed at CRG at all temperatures. The spectral shapes also differed: February spectra were more log-linear, whereas July spectra exhibited a sharp increase in concentration before -15 °C followed by a plateau, consistent with the influence of biological INPs (Creamean et al., 2019). This is notable given that Baltimore is an urban



311

312313

314

315316

317

318

319

320

321322

323324

325

326

327328

329330

331332

333

334

335336



environment, yet it may still be influenced by biological activity linked to ice nucleation activity, which has been observed in other urban environments (Cabrera-Segoviano et al., 2022; Tobo et al., 2020; Yadav et al., 2019). Warmer freezing temperatures were reached in February due to larger sampling volumes (Table 1), with detection up to -7 °C compared to -11 °C in July. In July, the flights on 22 Jul, 26 Jul, and the lowest (53–423 m) and highest (618–1062 m) altitude ranges on 28 Jul had statistically significant differences (p = 0.04, 0.02, and 0.05, respectively). During all three cases, higher INP concentrations were observed at the lower altitude ranges than the upper ranges, which was the opposite of the February observations.

Figure 7, similar to Figure 6, presents results from BNF flights across four months in 2025. In March, INPs were limited to relatively colder temperatures (≤ −14 °C)—even though the highest volumes of air were sampled compared to other months at BNF (Table 1)—and no statistically significant differences were observed between altitude levels on any day (p > 0.10). In April, only one day included two altitude levels, which again showed no statistically significant difference (p = 0.77). Generally, April exhibited average concentrations comparable to those observed in March (13 and 10 L<sup>-1</sup> at -25 °C, respectively). By the end of April, a single sample was collected over the full flight from ground level to 850 m, and concentrations began to increase toward the warmer end of the spectrum. May involved one flight towards the end of the month at two altitude levels with no statistical difference (p = 0.42) and were similar in concentration to March and April on average (12 L<sup>-1</sup> at -25 °C). Although the 1 June samples did not show a statistically significant difference (p = 0.14), the higher altitude range exhibited an order of magnitude higher INP concentration than the lower range (42 versus 4 L<sup>-1</sup> at – 25 °C). Later in June, concentrations increased at warmer freezing temperatures, and a statistically significant difference was observed during the 15 June flight (p = 0.00), with the lower altitude range showing higher INP concentrations (41 versus 5 L<sup>-1</sup> at -25 °C), opposite to the pattern observed earlier in the month. This increase suggests that as summer approaches, biological activity in the forest likely intensifies, producing biological INPs active at warmer freezing temperatures as evidenced by the spectral shape (Creamean et al., 2019). This is also consistent with observations of increased INPs and bioaerosols during summer in other forested regions (Petersson Sjögren et al., 2023; Schneider et al., 2021; Schumacher et al., 2013). Combined with CRG, these results highlight highly variable vertical and seasonal trends in INP concentrations at a single location, as captured by PUFIN and processed offline with the INS, yielding publicly available data for further exploration by the research community.





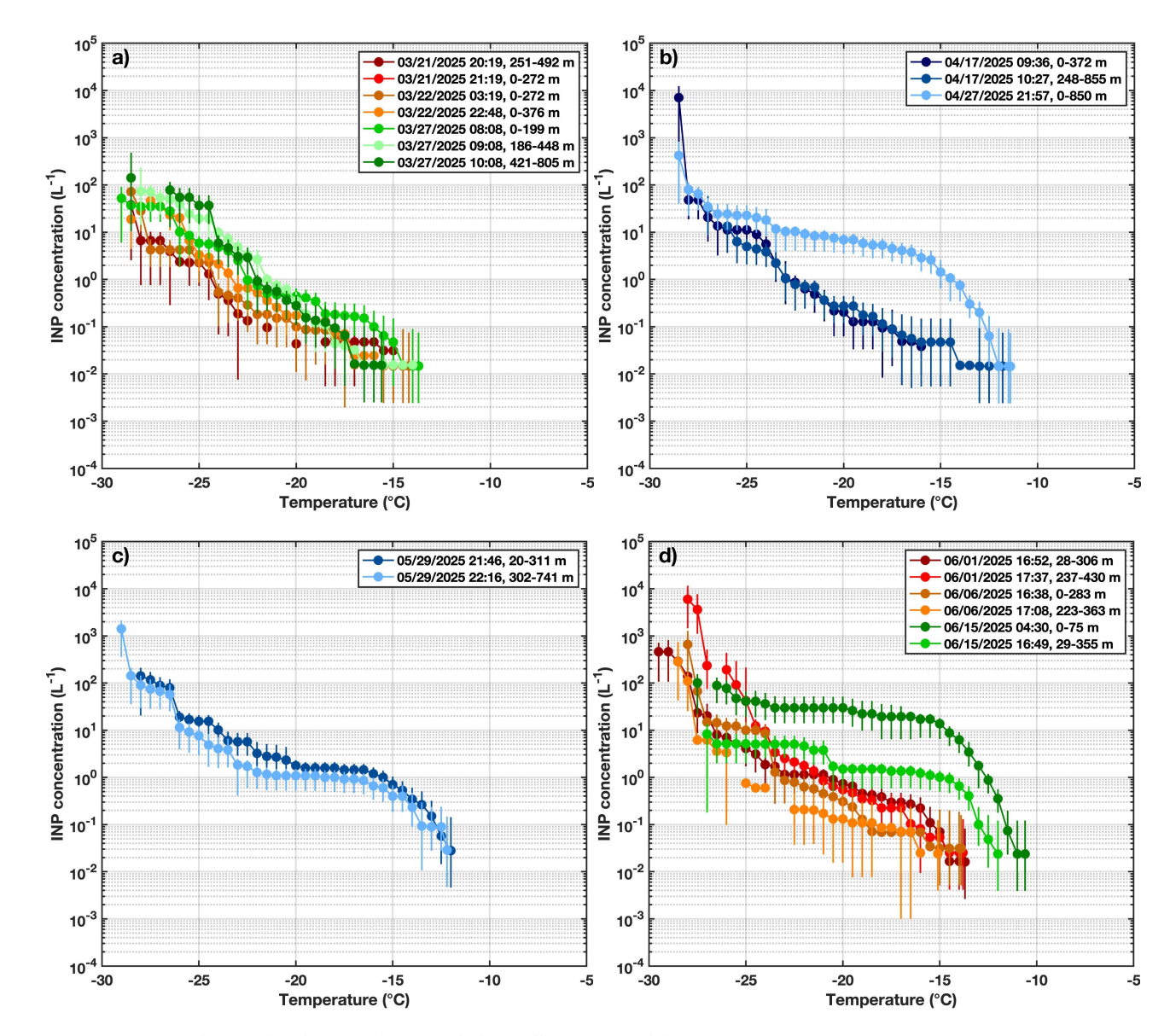


Figure 7: Same as Figure 6, but for BNF in a) March, b) April, c) May, and d) June 2025.

Overall, the flights conducted to date demonstrate that PUFIN can collect sufficient aerosol loadings to capture concentrations as low as  $10^{-2}$  INP L<sup>-1</sup> in as little as 28 minutes (equivalent to ~250 L of air; 4 minutes at 31 L of air is achievable but at a higher detection limit of  $10^{-1}$  INP L<sup>-1</sup>). For comparison, INP spectra from SGP and GUC TBS flights are shown in Figures S1 and S2, respectively, in which the same detection limit is achieved but from a longer sampling duration as discussed in Section 4.1. By comparison, ground-based ARM INP measurements are typically collected over 24 hours (~10000 to 30000 L of air), enabling lower detection limits of  $10^{-4}$  INP L<sup>-1</sup> (Creamean et al., 2025a). Although PUFIN cannot yet achieve such low concentrations, it provides valuable vertically-resolved INP measurements detectable at temperatures



347

348349

350

351352

353

354

355

356

357

358

359

360361

362

363

364

365

366367

368

369

370

371

372373

374

375



as warm as -7 °C from measurements thus far. Longer collection durations may further extend detection toward warmer temperatures, potentially above -7 °C. However, further testing in environments with known warm-temperature INPs, such as *Pseudomonas syringae*, is needed to determine whether PUFIN can adequately capture them.

# 4.3 Requesting PUFIN for future ARM TBS campaigns

Researchers interested in deploying PUFIN on an ARM TBS mission should first consider contacting the INP and TBS mentors (co-authors of this manuscript, Jessie Creamean and Darielle Dexheimer) to discuss the feasibility, timing, and logistical considerations of potential campaigns. Formal requests for PUFIN deployment are submitted through the ARM **TBS** proposal process, following the guidelines provided the **TBS** campaign website (https://www.arm.gov/guidance/campaign-guidelines/tbs). Proposals must target existing ARM observatories, adhere to specific submission deadlines, and include sufficient detail on desired sampling locations, altitudes, and measurement objectives. Both ARM-only and collaborative campaigns are supported. For example, researchers may propose joint ARM-EMSL FICUS (Facilities Integrating Collaborations for User Science) missions to deploy guest instruments, leverage specialized laboratory capabilities, and access additional resources to enhance the scientific output of the campaign (https://www.emsl.pnnl.gov/proposals/type/ficus-program). Detailed information on proposal requirements, timelines, and eligible instruments is provided on the ARM TBS guidance webpage.

#### 5 Summary

This paper introduces PUFIN (Profiling Upper altitudes For Ice Nucleation), a robust INP sampling system developed for routine deployment on the DOE ARM TBS platform. INPs, though present at concentrations orders of magnitude lower than CCN, exert a strong influence on cloud microphysics, lifetime, and radiative properties, particularly in mixed-phase clouds. Accurate representation of INPs in weather and climate models requires knowledge of their vertical distribution, which is often not captured by surface-based measurements or short-duration crewed aircraft observations. Small, flexible platforms such as TBS allow multi-hour, vertically-resolved sampling at targeted altitudes below, within, and above clouds.

PUFIN collects filters at up to three altitudes plus a field blank per flight, and all operations are fully ground-controlled. The collected samples are processed offline using the INS at Colorado State University, producing cumulative INP spectra across subzero temperatures. Recent deployments in Baltimore, Maryland (CRG) and Bankhead National Forest, Alabama (BNF) demonstrate that PUFIN can detect INP concentrations as low as  $\sim 10^{-3}$  L<sup>-1</sup> in as little as 28 minutes, a substantial improvement over the older ARM TBS INP sampling system and enabling multiple altitude profiles per flight. CRG data revealed notable vertical variability in INP concentrations likely linked to boundary layer stratification and aerosol transport, while BNF exhibited generally lower INP concentrations with limited vertical dependence.





376 All PUFIN-generated INP data are publicly available via the ARM Data Center, and researchers can request PUFIN 377 deployment for future TBS campaigns, including collaborative missions at existing and future proposed ARM observatories. 378 Looking forward, expanding the use of PUFIN and similar systems as TBS operations become more routine would not only 379 provide more comprehensive assessments of vertical INP distributions but also capture seasonal variability in these profiles. 380 By providing high-resolution, vertically-stratified INP measurements, PUFIN enhances understanding of aerosol-cloud 381 interactions, informs representation of INPs in models, and supports studies of regional to global climate processes. 382 Data availability 383 TBSINP data are available from the DOE ARM Data Center (https://www.arm.gov/data) or Data Discovery portal 384 (https://adc.arm.gov/discovery/) under DOI https://doi.org/10.5439/2001041 (Creamean et al., 2024). PUFIN design drawing and parts list are available at https://github.com/ARM-Development/TBS-INP-Design. 385 386 **Author contributions** 387 JMC and AT conceptualised the INP mentor program. JMC, CCH, DD, and BTMH designed the TBSINP sampler, while 388 BTMH built it. DD, CL, and CR were responsible for TBS deployments at ARM sites. CCH and MV conducted the sample 389 and data analysis for the TBSINP data that are publicly-available for download from the DOE ARM Data Center. All authors 390 contributed to the writing of this manuscript. 391 **Competing interests** 392 None of the authors has any competing interests. 393 **Disclaimer** 394 Publisher's note: Copernicus Publications remains neutral with regard to jurisdictional claims made in the text, published 395 maps, institutional affiliations, or any other geographical representation in this paper. While Copernicus Publications makes 396 every effort to include appropriate place names, the final responsibility lies with the authors. 397 Acknowledgements 398 This work was supported by the Office of Biological and Environmental Research within the U.S. Department of Energy 399 (DOE) through the Atmospheric Radiation Measurement (ARM) user facility. JMC, CCH, and MV received support under 400 DOE contract no. DE-0F-60173. We gratefully acknowledge James Mather for his invaluable support in the development





- 401 and implementation of the INP program. We also extend our sincere thanks to the ARM site staff for their significant
- assistance with instrument installation, sample collection, and logistics. We gratefully acknowledge Thomas C. J. Hill for
- 403 his foundational role as co-mentor alongside JMC during the inception of this program, and for his enduring guidance and
- 404 expertise. He is now enjoying a well-earned retirement in Australia. ChatGPT was used to assist in editing and improving
- the wording of this manuscript.

# Financial support

407 This research has been supported by Argonne National Laboratory for the DOE under contract DE-0F-60173.

### 408 References

406

- 409 Agresti, A. and Coull, B. A.: Approximate Is Better than "Exact" for Interval Estimation of Binomial Proportions, Am. Stat.,
- 410 52, 119, https://doi.org/10.2307/2685469, 1998.
- Barry, K. R., Hill, T. C. J., Jentzsch, C., Moffett, B. F., Stratmann, F., and DeMott, P. J.: Pragmatic protocols for working
- 412 cleanly when measuring ice nucleating particles, Atmospheric Res., 250, 105419,
- 413 https://doi.org/10.1016/j.atmosres.2020.105419, 2021.
- Barry, K. R., Hill, T. C. J., Nieto-Caballero, M., Douglas, T. A., Kreidenweis, S. M., DeMott, P. J., and Creamean, J. M.:
- 415 Active thermokarst regions contain rich sources of ice nucleating particles, EGUsphere, 1-19,
- 416 https://doi.org/10.5194/egusphere-2023-1208, 2023.
- Beall, C. M., Stokes, M. D., Hill, T. C., DeMott, P. J., DeWald, J. T., and Prather, K. A.: Automation and heat transfer
- characterization of immersion mode spectroscopy for analysis of ice nucleating particles, Atmospheric Meas. Tech., 10,
- 419 2613–2626, https://doi.org/10.5194/amt-10-2613-2017, 2017.
- 420 Böhmländer, A., Lacher, L., Brus, D., Doulgeris, K.-M., Brasseur, Z., Boyer, M., Kuula, J., Leisner, T., and Möhler, O.: A
- 421 novel aerosol filter sampler for measuring the vertical distribution of ice-nucleating particles via fixed-wing uncrewed aerial
- 422 vehicles, Atmospheric Meas. Tech., 18, 3959–3971, https://doi.org/10.5194/amt-18-3959-2025, 2025.
- 423 Burrows, S. M., McCluskey, C. S., Cornwell, G., Steinke, I., Zhang, K., Zhao, B., Zawadowicz, M., Raman, A., Kulkarni,
- 424 G., China, S., Zelenyuk, A., and DeMott, P. J.: Ice-Nucleating Particles That Impact Clouds and Climate: Observational and
- 425 Modeling Research Needs, Rev. Geophys., 60, e2021RG000745, https://doi.org/10.1029/2021RG000745, 2022.
- 426 Cabrera-Segoviano, D., Pereira, D. L., Rodriguez, C., Raga, G. B., Miranda, J., Alvarez-Ospina, H., and Ladino, L. A.: Inter-
- 427 annual variability of ice nucleating particles in Mexico city, Atmos. Environ., 273, 118964,
- 428 https://doi.org/10.1016/j.atmosenv.2022.118964, 2022.
- 429 Chatziparaschos, M., Myriokefalitakis, S., Kalivitis, N., Daskalakis, N., Nenes, A., Gonçalves Ageitos, M., Costa-Surós, M.,
- 430 Pérez García-Pando, C., Vrekoussis, M., and Kanakidou, M.: Assessing the global contribution of marine aerosols, terrestrial
- 431 bioaerosols, and desert dust to ice-nucleating particle concentrations, Atmospheric Chem. Phys., 25, 9085–9111,
- 432 https://doi.org/10.5194/acp-25-9085-2025, 2025.





- Cornwell, G. C., Steinke, I., Lata, N. N., Zelenyuk, A., Kulkarni, G., Pekour, M., Perkins, R., Levin, E. J. T., China, S.,
- DeMott, P. J., and Burrows, S. M.: Enrichment of Phosphates, Lead, and Mixed Soil-Organic Particles in INPs at the
- Southern Great Plains Site, J. Geophys. Res. Atmospheres, 129, e2024JD040826, https://doi.org/10.1029/2024JD040826,
- 436 2024.
- 437 Creamean, J., Hill, T., Hume, C., and Devadoss, T.: Ice Nucleation Spectrometer (INS) Instrument Handbook, U.S.
- 438 Department of Energy, Atmospheric Radiation Measurement user facility, Richland, Washington, 2024.
- Creamean, J. M., Primm, K. M., Tolbert, M. A., Hall, E. G., Wendell, J., Jordan, A., Sheridan, P. J., Smith, J., and Schnell,
- 440 R. C.: HOVERCAT: a novel aerial system for evaluation of aerosol-cloud interactions, Atmospheric Meas. Tech., 11, 3969-
- 3985, https://doi.org/10.5194/amt-11-3969-2018, 2018.
- 442 Creamean, J. M., Mignani, C., Bukowiecki, N., and Conen, F.: Using freezing spectra characteristics to identify ice-
- 443 nucleating particle populations during the winter in the Alps, Atmospheric Chem. Phys., 19, 8123-8140,
- 444 https://doi.org/10.5194/acp-19-8123-2019, 2019.
- 445 Creamean, J. M., de Boer, G., Telg, H., Mei, F., Dexheimer, D., Shupe, M. D., Solomon, A., and McComiskey, A.: Assessing
- the vertical structure of Arctic aerosols using balloon-borne measurements, Atmospheric Chem. Phys., 21, 1737–1757,
- 447 https://doi.org/10.5194/acp-21-1737-2021, 2021.
- 448 Creamean, J. M., Hume, C. C., Vazquez, M., and Theisen, A.: Long-term measurements of ice nucleating particles at
- 449 Atmospheric Radiation Measurement (ARM) sites worldwide, Earth Syst. Sci. Data Discuss., 1-31,
- 450 https://doi.org/10.5194/essd-2025-352, 2025a.
- 451 Creamean, J. M., L. A. Miller, M. van Pinxteren, O. Crabeck, N. S. Steiner, L. Marelle, I. Deschepper, R. Lapere, A. Leon-
- 452 Marcos, K. A. Pratt, J. L. Thomas, A. Da Silva, M. M. Frey, I. Peeken, H. Horowitz, M. D. Willis, and R. Price: Polar primary
- aerosols across the ocean-sea ice-snow-atmosphere interface: from sources to impacts, Elem. Sci. Anthr., in revision, 2025b.
- DeMott, P. J., Hill, T. C. J., Petters, M. D., Bertram, A. K., Tobo, Y., Mason, R. H., Suski, K. J., McCluskey, C. S., Levin,
- 455 E. J. T., Schill, G. P., Boose, Y., Rauker, A. M., Miller, A. J., Zaragoza, J., Rocci, K., Rothfuss, N. E., Taylor, H. P., Hader,
- 456 J. D., Chou, C., Huffman, J. A., Pöschl, U., Prenni, A. J., and Kreidenweis, S. M.: Comparative measurements of ambient
- 457 atmospheric concentrations of ice nucleating particles using multiple immersion freezing methods and a continuous flow
- diffusion chamber, Atmospheric Chem. Phys., 17, 11227–11245, https://doi.org/10.5194/acp-17-11227-2017, 2017.
- Dexheimer, D., Whitson, G., Cheng, Z., Sammon, J., Gaustad, K., Mei, F., and Longbottom, C.: Tethered Balloon System
- 460 (TBS) Instrument Handbook, https://doi.org/10.2172/1415858, 2024.
- 461 Feldman, D. R., Aiken, A. C., Boos, W. R., Carroll, R. W. H., Chandrasekar, V., Collis, S., Creamean, J. M., Boer, G. de,
- 462 Deems, J., DeMott, P. J., Fan, J., Flores, A. N., Gochis, D., Grover, M., Hill, T. C. J., Hodshire, A., Hulm, E., Hume, C. C.,
- Jackson, R., Junyent, F., Kennedy, A., Kumjian, M., Levin, E. J. T., Lundquist, J. D., O'Brien, J., Raleigh, M. S., Reithel, J.,
- Rhoades, A., Rittger, K., Rudisill, W., Sherman, Z., Siirila-Woodburn, E., Skiles, S. M., Smith, J. N., Sullivan, R. C., Theisen,
- 465 A., Tuftedal, M., Varble, A. C., Wiedlea, A., Wielandt, S., Williams, K., and Xu, Z.: The Surface Atmosphere Integrated
- 466 Field Laboratory (SAIL) Campaign, https://doi.org/10.1175/BAMS-D-22-0049.1, 2023.
- 467 Griesche, H. J., Ohneiser, K., Seifert, P., Radenz, M., Engelmann, R., and Ansmann, A.: Contrasting ice formation in Arctic
- 468 clouds: surface-coupled vs. surface-decoupled clouds, Atmospheric Chem. Phys., 21, 10357-10374,
- 469 https://doi.org/10.5194/acp-21-10357-2021, 2021.





- 470 Guy, H., Martin, A. S., Olson, E., Brooks, I. M., and Neely III, R. R.: Measurement report: In situ vertical profiles of below-
- 471 cloud aerosol over the central Greenland Ice Sheet, Atmospheric Chem. Phys., 24, 11103-11114,
- 472 https://doi.org/10.5194/acp-24-11103-2024, 2024.
- 473 Hill, T. C. J., DeMott, P. J., Tobo, Y., Fröhlich-Nowoisky, J., Moffett, B. F., Franc, G. D., and Kreidenweis, S. M.: Sources
- of organic ice nucleating particles in soils, Atmospheric Chem. Phys., 16, 7195–7211, https://doi.org/10.5194/acp-16-7195-
- 475 2016, 2016.
- 476 Hiranuma, N., Augustin-Bauditz, S., Bingemer, H., Budke, C., Curtius, J., Danielczok, A., Diehl, K., Dreischmeier, K.,
- Ebert, M., Frank, F., Hoffmann, N., Kandler, K., Kiselev, A., Koop, T., Leisner, T., Möhler, O., Nillius, B., Peckhaus, A.,
- Rose, D., Weinbruch, S., Wex, H., Boose, Y., DeMott, P. J., Hader, J. D., Hill, T. C. J., Kanji, Z. A., Kulkarni, G., Levin, E.
- J. T., McCluskey, C. S., Murakami, M., Murray, B. J., Niedermeier, D., Petters, M. D., O'Sullivan, D., Saito, A., Schill, G.
- P., Tajiri, T., Tolbert, M. A., Welti, A., Whale, T. F., Wright, T. P., and Yamashita, K.: A comprehensive laboratory study
- 481 on the immersion freezing behavior of illite NX particles: a comparison of 17 ice nucleation measurement techniques,
- 482 Atmospheric Chem. Phys., 15, 2489–2518, https://doi.org/10.5194/acp-15-2489-2015, 2015.
- Kanji, Z. A., Ladino, L. A., Wex, H., Boose, Y., Burkert-Kohn, M., Cziczo, D. J., and Krämer, M.: Overview of ice nucleating
- 484 particles, Meteor Monogr, 58, 1.1-1.33, https://doi.org/10.1175/AMSMONOGRAPHS-D-16-0006.1, 2017.
- Knopf, D. A., Barry, K. R., Brubaker, T. A., Jahl, L. G., Jankowski, K. A., Li, J., Lu, Y., Monroe, L. W., Moore, K. A.,
- Rivera-Adorno, F. A., Sauceda, K. A., Shi, Y., Tomlin, J. M., Vepuri, H. S. K., Wang, P., Lata, N. N., Levin, E. J. T.,
- 487 Creamean, J. M., Hill, T. C. J., China, S., Alpert, P. A., Moffet, R. C., Hiranuma, N., Sullivan, R. C., Fridlind, A. M., West,
- 488 M., Riemer, N., Laskin, A., DeMott, P. J., and Liu, X.: Aerosol-Ice Formation Closure: A Southern Great Plains Field
- 489 Campaign, Bull. Am. Meteorol. Soc., 102, E1952–E1971, https://doi.org/10.1175/BAMS-D-20-0151.1, 2021.
- 490 Lacher, L., Adams, M. P., Barry, K., Bertozzi, B., Bingemer, H., Boffo, C., Bras, Y., Büttner, N., Castarede, D., Cziczo, D.
- J., DeMott, P. J., Fösig, R., Goodell, M., Höhler, K., Hill, T. C. J., Jentzsch, C., Ladino, L. A., Levin, E. J. T., Mertes, S.,
- Möhler, O., Moore, K. A., Murray, B. J., Nadolny, J., Pfeuffer, T., Picard, D., Ramírez-Romero, C., Ribeiro, M., Richter, S.,
- 493 Schrod, J., Sellegri, K., Stratmann, F., Swanson, B. E., Thomson, E. S., Wex, H., Wolf, M. J., and Freney, E.: The Puy de
- 494 Dôme ICe Nucleation Intercomparison Campaign (PICNIC): comparison between online and offline methods in ambient air,
- 495 Atmospheric Chem. Phys., 24, 2651–2678, https://doi.org/10.5194/acp-24-2651-2024, 2024.
- 496 Lonardi, M., Pilz, C., Akansu, E. F., Dahlke, S., Egerer, U., Ehrlich, A., Griesche, H., Heymsfield, A. J., Kirbus, B., Schmitt,
- 497 C. G., Shupe, M. D., Siebert, H., Wehner, B., and Wendisch, M.: Tethered balloon-borne profile measurements of
- 498 atmospheric properties in the cloudy atmospheric boundary layer over the Arctic sea ice during MOSAiC: Overview and
- 499 first results, Elem. Sci. Anthr., 10, 000120, https://doi.org/10.1525/elementa.2021.000120, 2022.
- McCluskey, C. S., Hill, T. C. J., Malfatti, F., Sultana, C. M., Lee, C., Santander, M. V., Beall, C. M., Moore, K. A., Cornwell,
- 501 G. C., Collins, D. B., Prather, K. A., Jayarathne, T., Stone, E. A., Azam, F., Kreidenweis, S. M., and DeMott, P. J.: A
- 502 Dynamic Link between Ice Nucleating Particles Released in Nascent Sea Spray Aerosol and Oceanic Biological Activity
- 503 during Two Mesocosm Experiments, J. Atmospheric Sci., 74, 151–166, https://doi.org/10.1175/JAS-D-16-0087.1, 2017.
- Mei, F., Zhang, Q., Zhang, D., Fast, J. D., Kulkarni, G., Pekour, M. S., Niedek, C. R., Glienke, S., Silber, I., Schmid, B.,
- 505 Tomlinson, J. M., Mehta, H. S., Mansoura, X., Cheng, Z., Vandergrift, G. W., Lata, N. N., China, S., and Zhu, Z.:
- 506 Measurement report: Vertically resolved atmospheric properties observed over the Southern Great Plains with the
- ArcticShark uncrewed aerial system, Atmospheric Chem. Phys., 25, 3425–3444, https://doi.org/10.5194/acp-25-3425-2025,
- 508 2025.





- 509 Mülmenstädt, J., Sourdeval, O., Delanoë, J., and Quaas, J.: Frequency of occurrence of rain from liquid-, mixed-, and ice-
- 510 phase clouds derived from A-Train satellite retrievals: RAIN FROM LIQUID- AND ICE-PHASE CLOUDS, Geophys. Res.
- 511 Lett., 42, 6502–6509, https://doi.org/10.1002/2015GL064604, 2015.
- Murray, B. J., Carslaw, K. S., and Field, P. R.: Opinion: Cloud-phase climate feedback and the importance of ice-nucleating
- 513 particles, Atmospheric Chem. Phys., 21, 665–679, https://doi.org/10.5194/acp-21-665-2021, 2021.
- Petersson Sjögren, M., Alsved, M., Šantl-Temkiv, T., Bjerring Kristensen, T., and Löndahl, J.: Measurement report:
- Atmospheric fluorescent bioaerosol concentrations measured during 18 months in a coniferous forest in the south of Sweden,
- 516 Atmospheric Chem. Phys., 23, 4977–4992, https://doi.org/10.5194/acp-23-4977-2023, 2023.
- 517 Pilz, C., Düsing, S., Wehner, B., Müller, T., Siebert, H., Voigtländer, J., and Lonardi, M.: CAMP: an instrumented platform
- for balloon-borne aerosol particle studies in the lower atmosphere, Atmospheric Meas. Tech., 15, 6889–6905,
- 519 https://doi.org/10.5194/amt-15-6889-2022, 2022.
- 520 Pilz, C., Lonardi, M., Egerer, U., Siebert, H., Ehrlich, A., Heymsfield, A. J., Schmitt, C. G., Shupe, M. D., Wehner, B., and
- Wendisch, M.: Profile observations of the Arctic atmospheric boundary layer with the BELUGA tethered balloon during
- 522 MOSAiC, Sci. Data, 10, 534, https://doi.org/10.1038/s41597-023-02423-5, 2023.
- Pilz, C., Cassano, J. J., de Boer, G., Kirbus, B., Lonardi, M., Pöhlker, M., Shupe, M. D., Siebert, H., Wendisch, M., and
- Wehner, B.: Tethered balloon measurements reveal enhanced aerosol occurrence aloft interacting with Arctic low-level
- 525 clouds, Elem. Sci. Anthr., 12, 00120, https://doi.org/10.1525/elementa.2023.00120, 2024.
- Pohorsky, R., Baccarini, A., Tolu, J., Winkel, L. H. E., and Schmale, J.: Modular Multiplatform Compatible Air
- 527 Measurement System (MoMuCAMS): a new modular platform for boundary layer aerosol and trace gas vertical
- measurements in extreme environments, Atmospheric Meas. Tech., 17, 731–754, https://doi.org/10.5194/amt-17-731-2024,
- 529 2024.
- Pohorsky, R., Baccarini, A., Brett, N., Barret, B., Bekki, S., Pappaccogli, G., Dieudonné, E., Temime-Roussel, B., D'Anna,
- 531 B., Cesler-Maloney, M., Donateo, A., Decesari, S., Law, K. S., Simpson, W. R., Fochesatto, J., Arnold, S. R., and Schmale,
- 532 J.: In situ vertical observations of the layered structure of air pollution in a continental high-latitude urban boundary layer
- during winter, Atmospheric Chem. Phys., 25, 3687–3715, https://doi.org/10.5194/acp-25-3687-2025, 2025.
- Porter, G. C. E., Sikora, S. N. F., Adams, M. P., Proske, U., Harrison, A. D., Tarn, M. D., Brooks, I. M., and Murray, B. J.:
- Resolving the size of ice-nucleating particles with a balloon deployable aerosol sampler: the SHARK, Atmospheric Meas.
- 536 Tech., 13, 2905–2921, https://doi.org/10.5194/amt-13-2905-2020, 2020.
- Porter, G. C. E., Adams, M. P., Brooks, I. M., Ickes, L., Karlsson, L., Leck, C., Salter, M. E., Schmale, J., Siegel, K., Sikora,
- 538 S. N. F., Tarn, M. D., Vüllers, J., Wernli, H., Zieger, P., Zinke, J., and Murray, B. J.: Highly active ice-nucleating particles
- 539 at the summer North Pole, J. Geophys. Res. Atmospheres, 127, e2021JD036059, https://doi.org/10.1029/2021JD036059,
- 540 2022.
- Pruppacher, H. R. and Klett, J. D.: Microphysics of Clouds and Precipitation, Springer Netherlands, Dordrecht,
- 542 https://doi.org/10.1007/978-0-306-48100-0, 2010.
- 543 Schneider, J., Höhler, K., Heikkilä, P., Keskinen, J., Bertozzi, B., Bogert, P., Schorr, T., Umo, N. S., Vogel, F., Brasseur, Z.,
- Wu, Y., Hakala, S., Duplissy, J., Moisseev, D., Kulmala, M., Adams, M. P., Murray, B. J., Korhonen, K., Hao, L., Thomson,
- 545 E. S., Castarède, D., Leisner, T., Petäjä, T., and Möhler, O.: The seasonal cycle of ice-nucleating particles linked to the
- abundance of biogenic aerosol in boreal forests, Atmospheric Chem. Phys., 21, 3899–3918, https://doi.org/10.5194/acp-21-
- 547 3899-2021, 2021.





- 548 Schnell, R. C. and Vali, G.: Biogenic Ice Nuclei: Part I. Terrestrial and Marine Sources, J. Atmospheric Sci., 33, 1554–1564,
- 549 https://doi.org/10.1175/1520-0469(1976)033%253C1554:BINPIT%253E2.0.CO;2, 1976.
- 550 Schumacher, C. J., Pöhlker, C., Aalto, P., Hiltunen, V., Petäjä, T., Kulmala, M., Pöschl, U., and Huffman, J. A.: Seasonal
- 551 cycles of fluorescent biological aerosol particles in boreal and semi-arid forests of Finland and Colorado, Atmospheric Chem.
- 552 Phys., 13, 11987–12001, https://doi.org/10.5194/acp-13-11987-2013, 2013.
- 553 Steiner, A. L.: Role of the Terrestrial Biosphere in Atmospheric Chemistry and Climate, Acc. Chem. Res., 53, 1260–1268,
- 554 https://doi.org/10.1021/acs.accounts.0c00116, 2020.
- 555 Storelymo, T.: Aerosol Effects on Climate via Mixed-Phase and Ice Clouds, Annu. Rev. Earth Planet. Sci., 45, 199–222,
- 556 https://doi.org/10.1146/annurev-earth-060115-012240, 2017.
- 557 Suski, K. J., Hill, T. C. J., Levin, E. J. T., Miller, A., DeMott, P. J., and Kreidenweis, S. M.: Agricultural harvesting emissions
- of ice-nucleating particles, Atmospheric Chem. Phys., 18, 13755–13771, https://doi.org/10.5194/acp-18-13755-2018, 2018.
- Tobo, Y., Uetake, J., Matsui, H., Moteki, N., Uji, Y., Iwamoto, Y., Miura, K., and Misumi, R.: Seasonal Trends of
- 560 Atmospheric Ice Nucleating Particles Over Tokyo, J. Geophys. Res. Atmospheres, 125, e2020JD033658,
- 561 https://doi.org/10.1029/2020JD033658, 2020.
- Vali, G.: Quantitative Evaluation of Experimental Results and the Heterogeneous Freezing Nucleation of Supercooled
- 563 Liquids, J. Atmospheric Sci., 28, 402–409, https://doi.org/10.1175/1520-
- 564 0469(1971)028%253C0402:QEOERA%253E2.0.CO;2, 1971.
- 565 Yaday, S., Venezia, R. E., Paerl, R. W., and Petters, M. D.: Characterization of Ice-Nucleating Particles Over Northern India,
- 566 J. Geophys. Res. Atmospheres, 124, 10467–10482, https://doi.org/10.1029/2019JD030702, 2019.
- Zinke, J., Salter, M. E., Leck, C., Lawler, M. J., Porter, G. C. E., Adams, M. P., Brooks, I. M., Murray, B. J., and Zieger, P.:
- The development of a miniaturised balloon-borne cloud water sampler and its first deployment in the high Arctic, Tellus B
- 569 Chem. Phys. Meteorol., 73, 1915614, https://doi.org/10.1080/16000889.2021.1915614, 2021.